Improving ASTER DEMs over glacierized terrain using photoclinometry

B. Raup, S.J.S. Khalsa

NSIDC, Boulder, Colorado, USA

http://nsidc.org/
http://glims.org/
braup@nsidc.org

ABSTRACT

Digital elevation models (DEMs) produced from ASTER stereo imagery over glacierized terrain frequently contain data voids, which some software packages fill by interpolation. Even when interpolation is applied, the results are often not accurate enough for studies of glacier thickness changes. DEMs are created by automatic cross-correlation between the image pairs, and rely on spatial variability in the digital number (DN) values for this process. Voids occur in radiometrically homogeneous regions, such as glacier accumulation areas covered with uniform snow, due to lack of correlation. The same property that leads to lack of correlation makes possible the derivation of elevation information from photoclinometry, also known as shape-from-shading. We demonstrate a technique to produce improved DEMs from ASTER data by combining the results from conventional cross-correlation DEM-generation software with elevation information produced from shape-from-shading in the accumulation areas of glacierized terrain. The resulting DEMs incorporate more information from the imagery, and the filled voids more accurately represent the glacier surface than simple filling by interpolation. This will allow for more accurate determination of glacier hypsometry and thickness changes, leading to better predictions of response to climate change.

Methods

We applied the photoclinometry (shape-from-shading) algorithm to a small sub-scene of an ASTER image of the Bering Glacier, Alaska, outlined in red in the small image in Figure 2. In Figure 1, the leftmost image is a red-green-blue composite image from ASTER bands 3, 2, and 1, and has been radiometrically stretched to bring out surface features. In Figure 2, the rightmost image is the calibrated DEM obtained from the following steps:

- We used PCI Geomatica to create a digital elevation model (DEM) from the ASTER stereo image pair. The unedited result is shown in Figure 1, middle panel. The data voids are visible as black regions, mostly seen on snow surfaces. Together with the DEM, PCI produces a "score channel" which indicates the quality of the DEM values on a per-cell basis.
- We applied the shape-from-shading algorithm as described in Liu (2003) to the small sub-scene of ASTER band 2 to the generate a relative DEM. The solar elevation and azimuth angles were 46.16° and 165.00° respectively.
- We fitted the relative DEM to the ASTER DEM by extracting non-void values from the ASTER DEM and the score channel in the sub-scene area. The score channel is in the range of 0 to 100. We applied a threshold of 10, setting any score values below that to 0, and then used the method of weighted least squares to fit the relative DEM to the ASTER DEM sub-scene to form the calibrated DEM. The fitting process done as follows. Z is the absolute vertical coordinate for the desired calibrated DEM (a vector with components z_i); X and Y are the horizontal coordinates, H is the relative elevation, and W is the sets of weights derived from the score channel, then we want to find the coefficients A, B, C, D in

$$z_i = A + Bx_i + Cy_i + Dh_i$$

A matrix equation is set up as

$$\begin{bmatrix} z_1 \\ z_2 \\ \vdots \\ z_n \end{bmatrix} = \begin{bmatrix} 1 & x_1 & y_1 & h_1 \\ 1 & x_2 & y_2 & h_2 \\ \vdots & \vdots & \vdots & \vdots \\ 1 & x_n & y_n & h_n \end{bmatrix} \begin{bmatrix} A \\ B \\ C \\ D \end{bmatrix} + \begin{bmatrix} \varepsilon_1 \\ \varepsilon_2 \\ \vdots \\ \varepsilon_n \end{bmatrix}$$

and solved by minimizing

$$\begin{aligned} s &= \sum_{n=1}^{n} \varepsilon_i^2 \\ &= \sum_{n=1}^{n} w_i (z_i - (A + Bx_i + Cy_i + Dh_i))^2 \end{aligned}$$

The coefficients are obtained as

$$[\ A \quad B \quad C \quad D\ ]^\top = (X^\top W X)^{-1} X^\top W Y$$

where $W = diag(w_1, w_2, \ldots, w_n)$ are weights derived from the score channel output from PCI.

- We then created the patched DEM by filling the ASTER DEM voids with the values from the calibrated DEM. The result is shown in the left panel of Figure 3.

Conclusions and Prospects

From this initial work, we can make a number of observations:

- This method will excel at filling data voids in ASTER DEMs over glacier accumulation areas that exhibit curvature, such as ice caps, flow divides, and saddles. In such cases, a simple spline interpolation will not capture the real surface, but a shape-from-shading DEM will. We will test this in future work.
- The unedited ASTER DEM appears noisy (as expected), and there is a 200 m mean difference between it and the National Elevation Dataset (NED) DEM in this small region of the accumulation area. The histogram in Figure 3 summarizes this. The ASTER DEM is higher, making it unlikely that the difference is due to real changes in the glacier. The origin of the error may be the fact that the ground control points we used in the generation of the ASTER DEM did not cover the full range of elevations.
- In a case like this one, where the snow surface was relatively flat, the coefficients resulting from the weighted least squares process are rather sensitive to the choice of ASTER DEM cells, due to the noisy nature of the ASTER DEM. Future work will quantify the resulting differences in the patched DEM, but preliminary work indicates that they are small.
- The photoclinometry software should be modified to operate on arbitrarily sized images that have had a mask applied to exclude parts of the image that contain rock outcrops, etc.

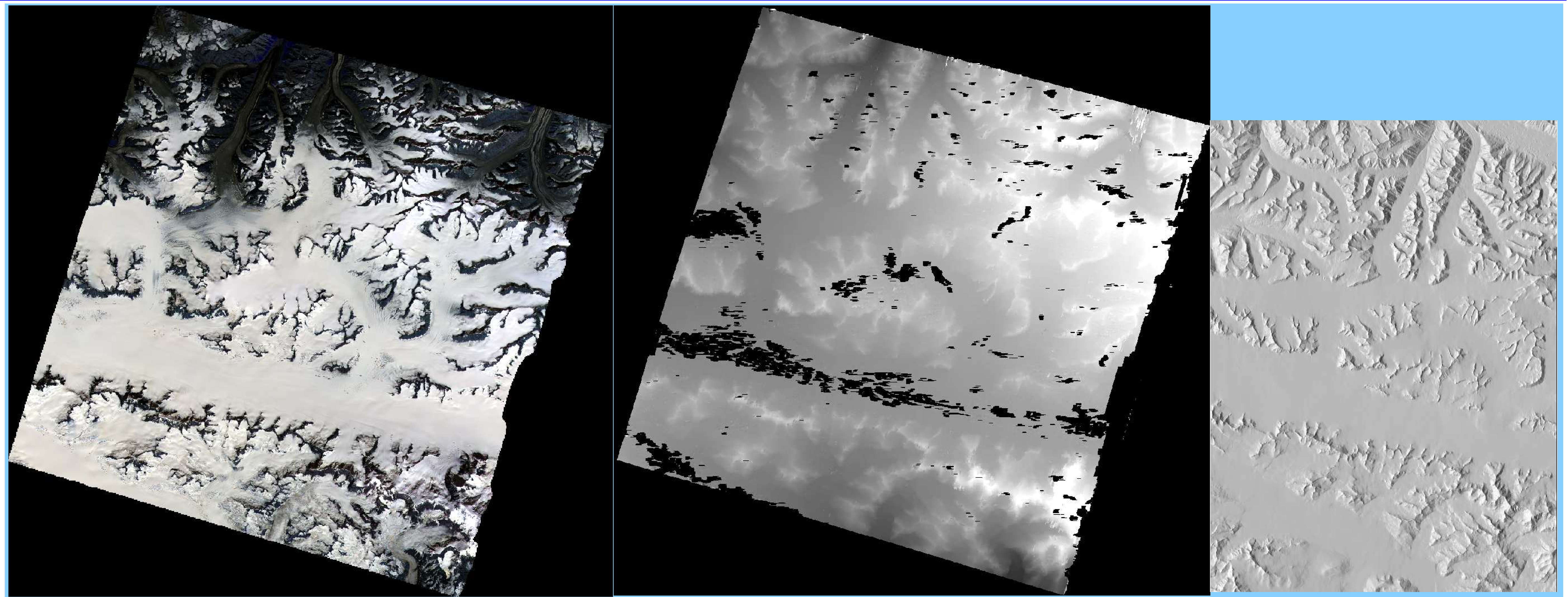

Figure 1: ASTER visible image (left) and its corresponding DEM (middle) covering part of the Bering Glacier, southern Alaska. Snowy areas in accumulation zones lead to holes in cross-correlation derived DEMs, but elevation information can be extracted using photoclinometry (shape-from-shading). For comparison, the image at right is a shade-relief map produced from the National Elevation Dataset (NED) digital elevation model (plotted at a slightly smaller scale).

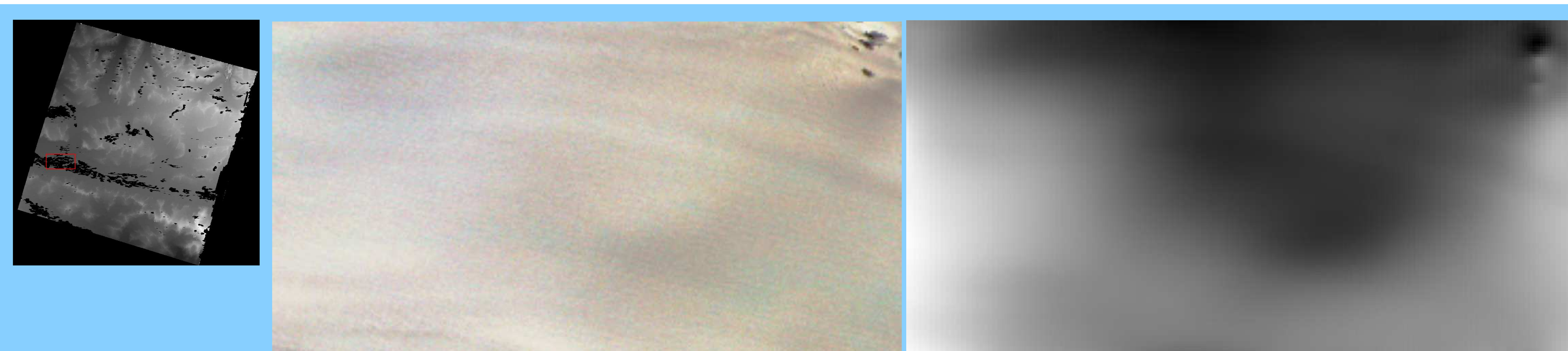

Figure 2: Detail of accumulation zone, located as shown in the red box at left. Middle panel is the visible image. The right panel is the calibrated DEM from photoclinometry.

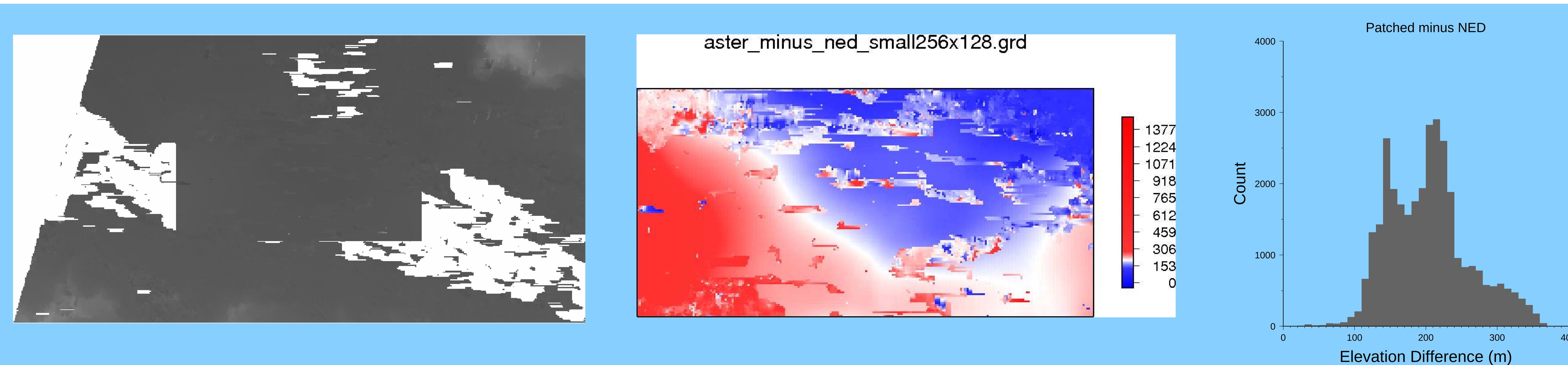

Figure 3: Left panel: The calibrated DEM is patched into the ASTER DEM. Middle panel: Difference between the patched ASTER DEM and the NED DEM. Both the variability of the ASTER DEM and the mean difference from the NED are apparent. Right panel: Histogram of the difference plotted in the middle panel.